THE JOURNAL OF BIOLOGICAL CHEMISTRY
Vol. 277, No. 45, Issue of November 8, pp. 43002–43010, 2002
Printed in U.S.A.

$GABA_A$ Receptor M2–M3 Loop Secondary Structure and Changes in Accessibility during Channel Gating*

Received for publication, June 25, 2002, and in revised form, September 3, 2002
Published, JBC Papers in Press, September 10, 2002, DOI 10.1074/jbc.M206321200

Amal K. Bera, Maya Chatav, and Myles H. Akabas‡

From the Departments of Physiology & Biophysics and of Neuroscience, Albert Einstein College of Medicine, Bronx, New York 10461

The γ-aminobutyric acid type A ($GABA_A$) receptor M2–M3 loop structure and its role in gating were investigated using the substituted cysteine accessibility method. Residues from α_1Arg-273 to α_1Ile-289 were mutated to cysteine, one at a time. $MTSET^+$ or $MTSES^-$ reacted with all mutants from α_1R273C to α_1Y281C, except α_1P277C, in the absence and presence of GABA. The $MTSET^+$ closed-state reaction rate was >1000 liters/mol-s at α_1N274C, α_1S275C, α_1K278C, and α_1Y281C and was <300 liters/mol-s at α_1R273C, α_1L276C, α_1V279C, α_1A280C, and α_1A284C. These two groups of residues lie on opposite sides of an α-helix. The fast reacting group lies on a continuation of the M2 segment channel-lining helix face. This suggests that the M2 segment α-helix extends about two helical turns beyond α_1N274 (20′), aligned with the extracellular ring of charge. At α_1S275C, α_1V279C, α_1A280C, and α_1A284C the reaction rate was faster in the presence of GABA. The reagents had no functional effect on the mutants from α_1A282C to α_1I289C, except α_1A284C. Access may be sterically hindered possibly by close interaction with the extracellular domain. We suggest that the M2 segment α-helix extends beyond the predicted extracellular end of the M2 segment and that gating induces a conformational change in and/or around the N-terminal half of the M2–M3 loop. Implications for coupling ligand-evoked conformational changes in the extracellular domain to channel gating in the membrane-spanning domain are discussed.

The $GABA_A$[1] receptors mediate inhibitory neurotransmission in the central nervous system (1). They are members of a gene superfamily that includes glycine, serotonin type 3, and nicotinic acetylcholine (ACh) receptors (2, 3). The $GABA_A$ receptors are a major target for drugs used for the induction and maintenance of general anesthesia and for the treatment of anxiety and epilepsy (1, 4).

The $GABA_A$ receptors are composed of five subunits arranged pseudo-symmetrically around the central channel axis. Each subunit has an extracellular N-terminal domain and a C-terminal domain with four transmembrane segments (M1–M4) that are largely α helical (5, 6). The putative ends of the membrane-spanning segments have been defined on the basis of hydrophobicity and sequence analysis (7, 8). There is, however, little experimental evidence to define precisely the ends of the helical membrane-spanning segments.

The subunits of this gene superfamily are built on a modular basis. The extracellular domain forms the agonist binding sites and determines the order of subunit assembly around the channel axis (6, 9–12). The C-terminal domain forms the ion channel that is largely lined by residues from the M2 membrane-spanning segments of each of the five subunits (13, 14). Support for the concept of modular design comes from the ability to generate functional chimeras between the GABA ρ receptor extracellular domain and the glycine receptor membrane-spanning domain, or between serotonin Type 3 and ACh α_7 receptors (15, 16). In addition, in invertebrates, a number of "chimeras" have evolved that combine extracellular domains that bind ACh, serotonin, or glutamate with a $GABA_A$-like, anion-selective, channel-forming, membrane-spanning domain (17, 18). The conformational changes by which ligand binding is coupled to movement of the channel gate are unknown.

Two regions of the membrane-spanning domain that might be involved in coupling to the extracellular domain are the pre-M1 region and the M2–M3 loop, the extracellular region that flanks the channel-lining M2 segment (Fig. 1). Depending on how the C-terminal end of M2 and the N-terminal end of M3 are defined, the M2–M3 loop is between 9 and 15 residues long. Only 3 to 5 residues would be necessary to form a β-turn between α helical M2 and M3 membrane-spanning segments. Several lines of evidence have implicated the M2–M3 loop in the signal transduction process. Mutations of three residues in the $GABA_A$ receptor γ_2 subunit, two in the M2 segment and one in the M2–M3 loop aligned with α_1Ala280, uncouples benzodiazepine binding in the extracellular domain from benzodiazepine potentiation of GABA-evoked currents (19). Mutations in the M2–M3 loop alter agonist efficacy in GABA, ACh, and glycine receptors (20–24). Naturally occurring mutations in the M2–M3 loop of glycine receptors cause startle disease (hyperekplexia) (25) and of the muscle acetylcholine receptors cause slow channel congenital myasthenic syndrome (22). The effect of many of these mutations is to uncouple or to reduce the coupling between ligand binding and channel gating (22–24). In α7/α3 chimeric nicotinic ACh receptors, mutation at Asp-266 in the M2–M3 loop of the α7 subunit exhibited poor response to different nicotinic agonists. Similar results were observed when the aligned residue in the ACh β4 subunit were mutated in α3/β4 ACh receptor (26). All these studies suggest that the M2–M3 loop may be involved in coupling conformational change between the two domains. There is, however, a paucity

* This work was supported by Grants NS30808, GM61925 and GM63266 from the National Institutes of Health. The costs of publication of this article were defrayed in part by the payment of page charges. This article must therefore be hereby marked "*advertisement*" in accordance with 18 U.S.C. Section 1734 solely to indicate this fact.

‡ To whom correspondence should be addressed: Dept. of Physiology & Biophysics, Albert Einstein College of Medicine, 1300 Morris Park Ave., Bronx, NY 10461. Tel.: 718-430-3360; Fax: 718-430-8819; E-mail: makabas@aecom.yu.edu.

[1] The abbreviations used are: GABA, γ-aminobutyric acid; ACh, acetylcholine; CFFR, calcium-free frog Ringer; MTS, methanethiosulfonate; $MTSES^-$, MTS-ethylsulfonate; $MTSET^+$, MTS-ethyltrimethylammonium; $5\text{-}HT_{3A}$, 5-hydroxytryptamine receptor type 3A; SCAM, substituted cysteine accessibility method; $pCMBS^-$, *p*-chloromercuribenzenesulfonate; ANOVA, analysis of variance.

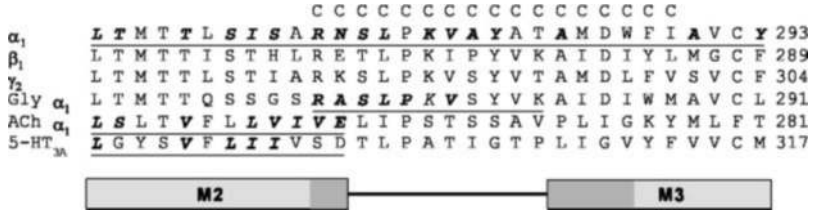

FIG. 1. **Aligned sequences of the M2–M3 loop and flanking regions of the rat GABA$_A$ receptor α_1, β_1, and γ_2 subunits, the human glycine α_1 subunit, the mouse muscle ACh α_1 subunit, and the mouse 5-HT$_{3A}$ subunit.** The *light gray bars* underneath indicate the M2 and M3 segments defined on the basis of hydropathy analysis. The *dark gray regions* indicate the uncertainty in the ends of the M2 and M3 segments based on sequence analysis. The residues in the GABA$_A$ α_1 subunit mutated to Cys in this study have a letter "*C*" over them in the *top line*. The *underlined regions* indicate positions studied by the substituted cysteine accessibility method in this or in other studies: data for GABA$_A$ receptor α_1 subunit (13, 33), glycine receptor (27), ACh receptor (38, 53), and 5-HT$_{3A}$ (39). Cysteines substituted for the residues in *boldface italic letters* are reactive with sulfhydryl reagents. *Numbers* at the *right* of *each row* indicate the amino acid number of the last residue shown. The first residue is the conserved leucine, the 9′ position in the M2 segment indexing system (35): GABA$_A$ α_1Leu-263, β_1Leu-259, γ_2Leu-274, glycine α_1Leu-261, ACh α_1Leu-251, and 5-HT$_{3A}$ Leu-287.

of data on the structure of the M2–M3 loop and little information on its structural dynamics during gating. Consistent with conformational change in this region, in the homo-pentameric glycine receptor, the water accessibility of residues in the N-terminal end of the M2–M3 loop increases in the presence of glycine (27).

To probe the structure and conformational changes that occur in the M2–M3 loop during channel gating, we used the substituted cysteine accessibility method (SCAM) (28, 29). This method assays the water-surface accessibility of engineered cysteine residues by their reactivity with water-soluble, charged sulfhydryl-specific reagents (29). The reagents used in this study were permanently charged derivatives of methanethiosulfonate (MTS), a positively charged derivative, MTS-ethyltrimethylammonium (MTSET$^+$), and a negatively charged derivative, MTS-ethylsulfonate (MTSES$^-$) (28). We mutated each of the α_1 subunit residues between α_1Arg-273 and α_1Ile-289 to cysteine (Cys), one at a time. We measured the reaction rates of the MTS reagents with the engineered Cys residues in the absence and in the presence of GABA. In the absence of GABA, the residues in the region between α_1Arg-273 and α_1Tyr-281 can be divided into two groups based on the MTSET$^+$ reaction rates. If this region is α helical, the two groups would lie on opposite faces of an α-helix. Additionally, we infer, based on increases in the reaction rates in the presence of GABA compared with the absence of GABA, that the region undergoes structural rearrangement during gating. At several positions in the M2–M3 loop the functional effects of covalent modification by MTSET$^+$ and MTSES$^-$ were similar suggesting the functional effects were due to steric factors rather than to electrostatic effects on permeating ions. In contrast, at two positions, α_1L276C and α_1A280C, the effect of modification was due to electrostatic interactions rather than steric effects possibly due to proximity with α_1Arg-273. The implications of these results for the structure of this region and its role in signal transduction are considered.

EXPERIMENTAL PROCEDURES

Molecular Biology—The cDNAs encoding the rat GABA$_A$ α_1, β_1, and γ_{2S} subunits in the pGEMHE vector were used (30). To ensure that the sulfhydryl reagents only reacted with the engineered Cys all of the endogenous Cys in membrane-spanning segments were mutated to other amino acids. Thus, "wild type" subunits had the following mutations: α_1 C233S and C292S; β_1 C288S; and γ_{2S} C244S, C303A, and C413A. Hereafter, these "Cys-minus" constructs will be referred to as wild type. The α_1 Cys-minus construct was used as the background for the M2–M3 loop mutations from α_1S275C to α_1I289C. Mutations were generated by PCR and confirmed by DNA sequencing (31). The α_1 wild type and all α_1 Cys mutants except α_1R273C, α_1N274C, and α_1S275C contained the FLAG epitope tag sequence inserted between residues 4 and 5 in the mature protein sequence. The β_1 subunit was tagged with the myc epitope sequence at the same site as described previously (14). Insertion of these epitope tags had no functional effect (32). α_1R273C and α_1N274C were in the wild type, endogenous-Cys-containing background. The M2 segment residues from α_1E249 to α_1N274 and the M3 segment residues from α_1A290 to α_1V306 were studied previously (13, 33). The 5′-capped cRNAs were made using standard procedures (14). Oocytes were injected with 50 nl of RNA (200 pg/nl) mixed in an equal ratio of α_1:β_1:γ_2. After injection, oocytes were incubated at 16–17 °C for 2–3 days in OR3 solution before use in electrophysiological experiments (14).

Residues in the M2 segment are referred to by an indexing number system that numbers a conserved positively charged amino acid, aligned with GABA$_A$ receptor α_1Arg-254, at the cytoplasmic end of M2 as the 0′ position and the residues (α_1Asn-274) aligned with the ACh receptor extracellular ring of charge (34) at the extracellular end of M2 as the 20′ position (35).

Electrophysiology—Two electrode voltage clamp experiments were performed at room temperature as described previously (13). Holding potential was −60 mV. The oocyte was continuously perfused at 6 ml/min with calcium-free frog Ringer (CFFR), containing 115 mM NaCl, 2.5 mM KCl, 1.8 mM $MgCl_2$, and 10 mM HEPES (pH 7.5). To determine the GABA EC_{50} concentration for wild type and the Cys mutants, concentration-response curves were generated by recording the currents elicited by increasing concentrations of GABA (Fig. 2). The GABA-induced currents for each GABA concentration were normalized relative to the maximal currents (I_{max}) and then plotted as a function of GABA concentration. The curves were fitted to the Hill equation, $I/I_{max} = ([c]^n)/(EC_{50}{}^n + [c]^n)$, where I_{max} is the maximum GABA-induced current, [*c*] is the GABA concentration, EC_{50} is the GABA concentration that gives half-maximal current, and n is the Hill coefficient, using Sigma Plot 2000 (SPSS Inc., Chicago, IL).

Sulfhydryl Reagents—We used the MTS derivatives MTSET$^+$ and MTSES$^-$ (Biotium, Inc., Haywood, CA). They add –SCH_2CH_2X onto the Cys where X is $N(CH_3)_3^+$ for MTSET$^+$ and SO_3^- for MTSES$^-$ (28).

Sulfhydryl Reagent Effects—Reaction of the MTS reagents with engineered Cys residues was assayed functionally by effects on GABA-induced currents. The effects of MTSET$^+$ and MTSES$^-$ were studied using the following protocol: two 10- to 20-s pulses of submaximal GABA concentration (EC_{20}-EC_{50}), designated as test pulses, were applied. Next, 1 mM MTSET$^+$ or 10 mM MTSES$^-$ ± near-saturating GABA concentration (5 times EC_{50}) was applied for 1 min. This was followed by two submaximal GABA test pulses. All applications were separated by 3- to 5-min washes with CFFR to allow complete recovery from desensitization. GABA-induced currents were stable before and after application of the sulfhydryl reagents. Experiments in which the peak currents of the two GABA test responses were not within 5% were discarded. The percentage effects of the sulfhydryl-specific reagents were calculated using the following equation: $[(I_{final}/I_{initial}) - 1] \times 100$. I_{final} designates the average peak current of the two test pulses after MTS reagent application, and $I_{initial}$ is the average peak current of the two initial GABA test pulses. To avoid MTS reagent hydrolysis, 100 mM stocks were made in distilled water each day, kept on ice, and diluted into CFFR immediately before use (29).

Data are presented as mean ± S.E. of at least three observations. All experiments were performed in at least two separate batches of oocytes from different frogs. Statistical significance of effects was determined by one-way analysis of variance (ANOVA) using the Dunnett post hoc test with wild type as control. $p < 0.05$ was considered significant.

It is important to recognize that MTS-reactive residues were identified based on functional effects of modification. Functional effects were determined by the statistical significance of the effect on a mutant

relative to the effect on wild type. For some mutants the average effect following MTS reagent application was small. Whether such an effect was statistically significant depended, in part, on the stringency of the one-way ANOVA post hoc test used. For example, in our previous work on the α_1 M3 segment, using the Student-Newman-Kuels post hoc test to determine significance, the effect of pCMBS$^-$ applied in the presence of GABA was significant at six residues: α_1A290C, α_1Y293C, α_1F297C, α_1A299C, α_1L300C, and α_1E302C. With the less stringent Duncan post hoc test, an additional residue α_1F295C was judged to be reactive with pCMBS$^-$ applied in the presence of GABA (33). The choice of post hoc test is, unfortunately, somewhat arbitrary. Thus, for Cys mutants where the effects of complete reaction are small, it may be difficult to determine whether reaction has occurred.

For screening experiments 1 mM MTSET$^+$ was applied for 1 min. This combination of time and concentration limits our ability to detect reactive residues. For a given mutant, based on the variability of responses, application of a reagent must cause a net change in current greater than ~30% to be statistically significantly different than wild type by a one-way ANOVA (for n between 3 and 6). Thus, if complete reaction caused 100% inhibition of the GABA-induced current, with a detection threshold of 30% effect and the MTSET$^+$ reaction conditions of 1 mM applied for 1 min, the slowest reaction rate that we can detect must have a second order reaction rate constant of >6 liters/mol-s. To place this in context, the second order rate constant for MTSET$^+$ reaction with 2-mercaptoethanol in solution at pH 7.0 is 2.1×10^5 liters/mol-s (29).

Measurement of Reaction Rates—The reaction rate of MTS reagents with engineered Cys were determined by the method described previously (36). A test pulse of GABA was applied to monitor the GABA-induced current. MTS reagents (1 μM to 1 mM) were applied with or without GABA for 10–60 s. The MTS reagent concentration was constant during an experiment and in vast molar excess to the number of Cys on the oocyte surface. After washing for 3–5 min, a second test pulse of GABA was applied and the peak current was measured. The brief pulses of reagent alternating with GABA test pulses continued until the reaction saturated, as observed by the plateau of the GABA test-pulse current magnitude. The magnitude of GABA-induced, test-pulse currents was normalized, relative to the current induced by GABA test pulses before exposure to the MTS reagents. The normalized currents were plotted as a function of cumulative exposure time to the MTS reagents. Using Prism 3 software (GraphPad Software, Inc., San Diego, CA) the curves were fitted with single- or double-exponential equations. The F-test was used to determine whether the double-exponential fit was significantly better than the single-exponential fit. In all cases, except α_1A280C in the presence of GABA, the best fit was obtained with a single-exponential function. The pseudo-first-order rate constant, obtained from the exponential fit, was divided by the molar concentration of MTS reagents to give the second order reaction rate constant. At most positions the pseudo-first order reaction rates were determined using at least two different concentrations of MTS reagent. Similar second order rates were obtained in all cases consistent with the reaction being a simple bimolecular reaction.

RESULTS

Characterization of Cysteine Substitution Mutants—Oocytes expressing each of the Cys substitution mutants displayed GABA-evoked currents. This indicated that the mutations were tolerated and yielded functional channels. The GABA EC_{50} values for the wild type and the mutants were determined (Table I and Fig. 2). Five mutants, α_1L276C, α_1P277C, α_1K278C, α_1D286C, and α_1F288C, had statistically significant increases in GABA EC_{50} (Table I). The Hill coefficient for wild type was 1.5, whereas for the mutants it ranged from 0.9 to 1.7. For wild type the average maximal current (I_{max}) was −4034 ± 359 nA (n = 28) at a holding potential of −60 mV. The I_{max} for the mutants ranged from −206 ± 41 nA (α_1D286C) to −3496 ± 236 nA (α_1I289C) (Table I). For three mutants, α_1A282C, α_1D286C, and α_1F288C, I_{max} was only 5–8% of the wild type I_{max}. The currents, however, were sufficiently large for our experiments.

Effect of MTSET$^+$—We studied the sensitivity to MTSET$^+$ of wild type and Cys substitution mutants both in the absence and in the presence of GABA. In the absence of GABA, the channels are in the closed state most of the time. Application of 1 mM MTSET$^+$ for 1 min irreversibly potentiated the GABA test pulse current amplitude for the mutants α_1R273C, α_1N274C, α_1S275C, α_1L276C, α_1V279C, and α_1A284C (Figs. 3 and 4*A*). The GABA-induced currents of the mutant α_1Y281C were significantly reduced after exposure to MTSET$^+$ (Fig. 4*A*). MTSET$^+$ application to wild type receptors and the other Cys mutants caused no functional effects (Fig. 4*A*). At α_1L276C the GABA-induced currents following MTSET$^+$ treatment in the absence of GABA were potentiated by 24%, however, this was not statistically significant.

In the presence of GABA the channels undergo transitions between the open, desensitized, and closed states. Application of 1 mM MTSET$^+$ in the presence of GABA irreversibly potentiated the subsequent GABA test currents for the mutants α_1R273C, α_1N274C, α_1S275C, α_1K278C, α_1V279C, and α_1A284C (Fig. 4*B*). The subsequent GABA test currents were irreversibly inhibited for the mutant α_1Y281C (Fig. 4*B*). The mutant α_1K278C showed 56% potentiation of subsequent GABA-induced currents when modified in a closed state (Fig.

TABLE I
GABA EC_{50} of M2–M3 loop cysteine substitution mutants

Mutant	n	EC_{50}	Hill coefficient	I_{max}
		μM		nA
WT	5	10 ± 2[a]	1.5 ± 0.2[a]	4034 ± 359
R273C	3	12 ± 1	0.9 ± 0.1	2621 ± 302
N274C	3	5 ± 0.2	1.0 ± 0.1	3397 ± 423
S275C	3	3 ± 0.1	1.1 ± 0.1	2639 ± 146
L276C	3	138 ± 12[b]	1.7 ± 0.2	1190 ± 428
P277C	4	143 ± 17[b]	1.3 ± 0.5	1026 ± 112
K278C	6	51 ± 13[b]	1.2 ± 0.1	2745 ± 134
V279C	3	20 ± 5	1.0 ± 0.1	2633 ± 149
A280C	4	8 ± 2	1.4 ± 0.2	2932 ± 509
Y281C	3	9 ± 2	1.0 ± 0.2	2919 ± 216
A282C	3	42 ± 3	1.5 ± 0.6	292 ± 43
T283C	5	24 ± 4	1.2 ± 0.1	2470 ± 227
A284C	5	12 ± 1	1.6 ± 0.3	2403 ± 417
M285C	3	13 ± 1.5	1.3 ± 0.1	2597 ± 241
D286C	4	77 ± 17[b]	1.0 ± 0.1	206 ± 41
W287C	8	3 ± 0.5	1.2 ± 0.1	2699 ± 139
F288C	4	65 ± 3[b]	1.0 ± 0.1	257 ± 21
I289C	3	37 ± 8	1.4 ± 0.1	3496 ± 239

[a] Mean ± S.E.
[b] Statistically significantly different from WT by one-way ANOVA with Dunnett's post hoc test.

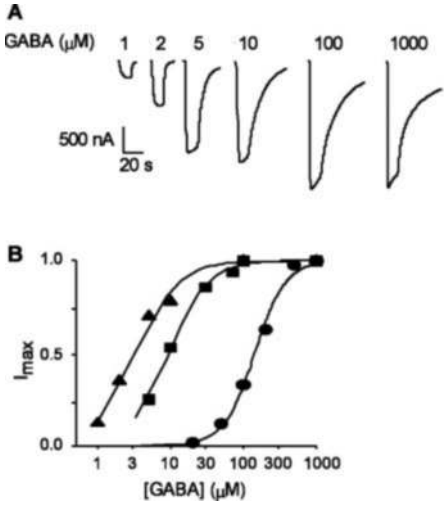

FIG. 2. **GABA concentration-response relationships.** *A*, currents from an oocyte expressing α_1W287C in response to the GABA concentration indicated above the trace. *B*, GABA concentration-response relationships from individual oocytes expressing α_1W287C (*triangles*), wild type (*squares*), and α_1L276C (*circles*). The *solid lines* are fits of the Hill equation to the data. Averaged data for GABA EC_{50}, n_H, and I_{max} for each mutant and wild type are presented in Table I.

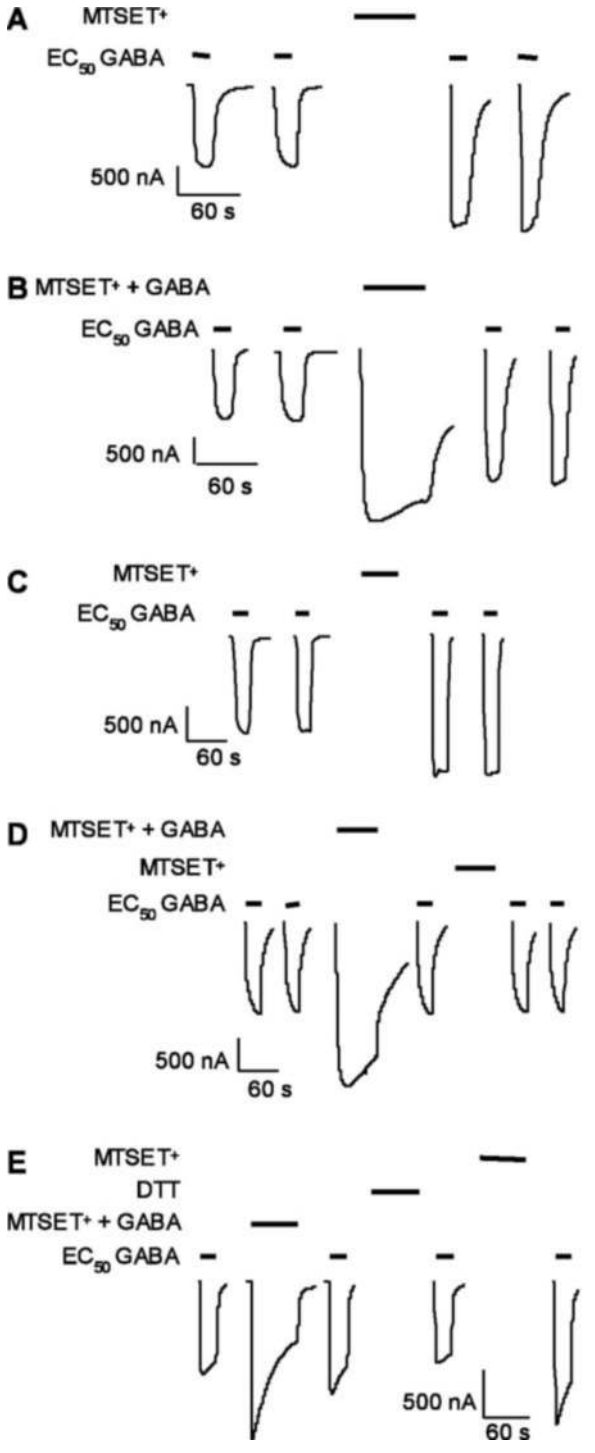

FIG. 3. **Effect of 1 mM $MTSET^+$ applied in the absence or in the presence of GABA on subsequent GABA-induced currents from oocytes expressing several of the Cys mutants.** *A*, $MTSET^+$ reacted with α_1V279C in the absence of GABA irreversibly potentiating subsequent GABA-induced currents. The current during application of $MTSET^+$ is not shown. *B*, $MTSET^+$ applied in the presence of 100 μM GABA (near-saturating concentration) reacted with α_1V279C potentiating the subsequent GABA-induced currents. In *A* and *B* EC_{50} GABA was 20 μM. *C*, at α_1K278C, $MTSET^+$ applied in the absence of GABA potentiated the subsequent GABA-induced currents. *D*, sequential application of $MTSET^+$ in the presence and then in the absence of GABA to an oocyte expressing α_1K278C$\beta_1\gamma_2$ receptors. $MTSET^+$ application in the presence of GABA had no effect on the subsequent EC_{50} GABA test current. Note the similar magnitude of the middle EC_{50} GABA test current and the initial test currents. Subsequent application of 1 mM $MTSET^+$ in the absence of GABA, which when applied first potentiated subsequent currents as in *panel C*, had no effect on subsequent EC_{50} GABA currents. This indicates that the engineered Cys reacted with $MTSET^+$ when it was first applied with GABA thereby blocking the possibility of reaction with the engineered Cys when $MTSET^+$ was applied a second time in the absence of GABA. In *D* the current during application of $MTSET^+$ alone is not shown. *E*, application of 10 mM dithiothreitol between the $MTSET^+$ applications reverses the ability of $MTSET^+$ that reacted in the presence of GABA to block the reaction during the second $MTSET^+$ application in the absence of GABA. Thus, in contrast to the absence of an effect by the second $MTSET^+$ application in *D*, now the second application causes potentiation of the subsequent currents. All *traces* are separated by 3- to 5-min washes with CFFR buffer to allow complete recovery from desensitization. The stability of the GABA-induced currents is indicated by the similar magnitudes of the pairs of GABA test currents before and after $MTSET^+$ application. Duration of application of GABA and 1 mM $MTSET^+$ is indicated by *bars* above the *traces*. Near-saturating GABA co-applied with $MTSET^+$ was 100 μM.

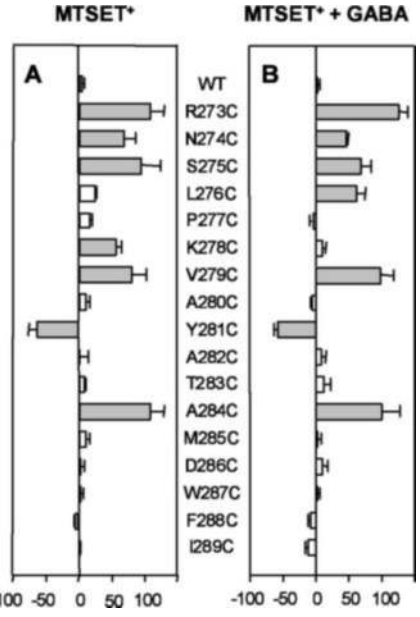

FIG. 4. **The average effect of a 1-min application of 1 mM $MTSET^+$ applied in the absence (*A*) and in the presence (*B*) of near-saturating GABA on wild type and the M2–M3 loop Cys mutants.** *Gray bars* indicate effects that are significantly different than the effect on wild type by a one-way ANOVA. Negative effect indicates inhibition and positive effect indicates potentiation of subsequent ~EC_{50} GABA-induced currents. At most reactive positions the subsequent currents were altered following application in the absence and presence of GABA, but at two positions subsequent currents were only affected following $MTSET^+$ application in the presence (α_1L276C) and in the absence (α_1K278C) of GABA.

3*C*) but did not show any effect when treated for 1 min with 1 mM $MTSET^+$ + GABA (Figs. 3*C*, 3*D*, and 4). To determine whether $MTSET^+$ reacted silently with α_1K278C in the presence of GABA, we applied $MTSET^+$ twice, first in the presence of GABA and then in the absence of GABA to the same oocytes (Fig. 3*D*). The ability of $MTSET^+$ to potentiate the subsequent GABA currents was eliminated by pretreatment with $MTSET^+$ + GABA. This inhibitory effect of pretreatment with $MTSET^+$ + GABA was reversed by application of 10 mM dithiothreitol between the $MTSET^+$ applications (Fig. 3*E*). This implies that, when applied in the presence of GABA, $MTSET^+$ covalently modified α_1K278C in a functionally silent manner. However, when applied in the absence of GABA, $MTSET^+$ modification altered subsequent channel function. The potentiation of GABA-induced currents by $MTSET^+$ treatment in the closed state was not reversed by subsequent co-application of GABA + $MTSET^+$ (data not shown). These experiments imply that the cysteines in both α subunits were reacting in both conditions.

A similar phenomenon was observed with the mutant α_1L276C. Modification by 1 mM $MTSET^+$ in the presence of

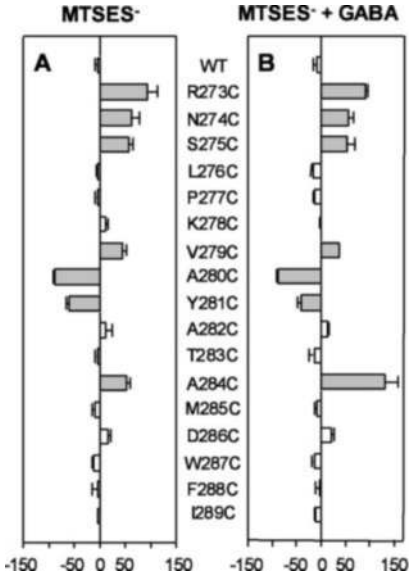

FIG. 5. **The average effect of a 1-min application of 10 mM MTSES$^-$ applied in the absence (*A*) and in the presence (*B*) of near-saturating GABA on wild type and the M2–M3 loop Cys mutants.** *Gray bars* indicate effects that are significantly different than the effect on wild type by a one-way ANOVA. Negative effect indicates inhibition, and positive effect indicates potentiation of subsequent EC_{50} GABA-induced currents. There are two notable differences between the effects follow application of MTSES$^-$ and MTSET$^+$. Note that at α_1A280C subsequent currents were inhibited following MTSES$^-$ application, but application of MTSET$^+$ had no effect on the subsequent currents in this mutant. Also, application of MTSES$^-$ had no effect on subsequent current at α_1L276C, but MTSET$^+$ had a significant effect.

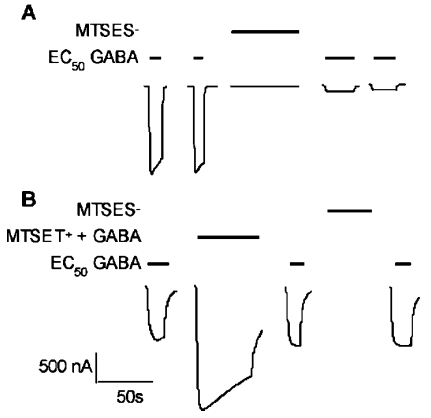

FIG. 6. **MTSET$^+$ reacts with α_1A280C but has no functional effect on the subsequent GABA-evoked currents.** *A*, a 1-min application of 10 mM MTSES$^-$ significantly inhibits the subsequent GABA-induced currents recorded from an oocyte expressing α_1A280C$\beta_1\gamma_2$ receptors. *B*, pre-application of 1 mM MTSET$^+$ in the presence of GABA has no effect on the subsequent GABA-induced currents but blocks the ability of a 1-min application of 10 mM MTSES$^-$ to inhibit the subsequent currents. This implies that MTSET$^+$ reacts with the engineered Cys but has no functional effect other than preventing subsequent reaction with MTSES$^-$.

GABA potentiated the subsequent GABA test pulses by 62% (Fig. 4). Application of 1 mM MTSET$^+$ in the absence of GABA did not have a statistically significant effect on the subsequent GABA-induced currents (Fig. 4*A*). Nevertheless, MTSET$^+$ reacted in the absence of GABA with the engineered Cys in α_1L276C, because it inhibited the ability of a subsequent application of MTSET$^+$ in the presence of GABA to potentiate GABA-induced currents (data not shown).

In our original SCAM analysis we reported that application of the MTS reagents had no functional effect on α_1R273C (13). In those experiments we used only saturating concentrations of GABA for the test pulses. Here we have used submaximal GABA concentrations for the test pulses. The functional effects of covalent modification by MTS reagents can alter single channel conductance or channel gating. If MTS modification only alters gating and not conductance, this may cause a shift in the GABA EC_{50} but should not affect maximal current elicited by saturating GABA. A shift in GABA EC_{50} will only be detected with submaximal GABA test pulses. Thus, the primary effect of α_1R273C modification by MTSET$^+$ must be a change in GABA EC_{50}.

Effect of MTSES$^-$—The reaction rate of sulfhydryls, such as 2-mercaptoethanol, with MTSES$^-$ (1.7×10^4 liters/mol-s) is about 10-fold lower than the rate with MTSET$^+$ (29). Therefore, for MTSES$^-$ screening experiments we used a 10-fold higher concentration of MTSES$^-$ than MTSET$^+$. A 1-min application of 10 mM MTSES$^-$, both in the absence and in the presence of GABA, significantly potentiated the subsequent GABA-induced currents of the mutants α_1R273C, α_1N274C, α_1S275C, α_1V279C, and α_1A284C and significantly inhibited the subsequent GABA-induced currents of the mutants α_1A280C and α_1Y281C (Figs. 5 and 6). MTSES$^-$ treatment of α_1L276C and α_1K278C did not have any functional effect on subsequent GABA-induced currents, but it blocked the effect of a subsequent application of MTSET$^+$ (data not shown). We inferred that these mutants reacted with MTSES$^-$, but the modification failed to exert any functional changes. Similarly, a 1-min application of MTSET$^+$ to α_1A280C had no functional effects other than blocking the inhibition induced by application of MTSES$^-$ (Fig. 6). Thus, MTSET$^+$ reacted silently with α_1A280C. These findings indicate that the lack of functional effects does not necessarily signify that a residue has not reacted and is not on the water-accessible surface.

MTSET$^+$ Reaction Rates with Cys Substitution Mutants—We measured the reaction rates of MTSET$^+$ with the accessible mutants in different receptor states, *i.e.* the closed state and in the presence of near-saturating GABA. Because the modification of α_1A280C by MTSET$^+$ had no functional effect, we determined the reaction rates with MTSES$^-$ (Fig. 7). The results are summarized in Table II. For the mutants α_1N274C, α_1S275C, α_1K278C, and α_1Y281C, the closed state MTSET$^+$ reaction rates were of similar magnitude, >1100 liters/mol-s. In contrast, for the mutants α_1R273C, α_1V279C, α_1A280C,[2] and α_1A284C the closed-state MTSET$^+$ reaction rates were <300 liters/mol-s.

In the presence of GABA, the MTSET$^+$ reaction rates with the residues α_1N274C, α_1S275C, α_1V279C, and α_1A284C were 3, 8, 7, and 2 times faster, respectively, than in the absence of GABA. The increase in reaction rate could result from changes in multiple factors. These include: 1) conformational changes either in this region or in a region contacting the M2–M3 loop that alters accessibility, 2) increased fractional time spent on the water-accessible surface, and/or 3) changes in local electrostatic potential that either alter the extent of ionization of the Cys or the local concentration of the MTS reagent. We cannot distinguish which of the above factors alters reactivity in the presence of GABA. The MTSET$^+$ reaction rate with the residue α_1Y281C was the same in the absence and presence of GABA, implying that the environment surrounding this residue did not change in the presence of agonist.

Only reaction with MTSES$^-$ had an effect on subsequent currents at α_1A280C. Applied in the closed state, the MTSES$^-$ reaction rate was 28 ± 5 liters/mol-s. When applied in the presence of GABA the plot of MTSES$^-$ cumulative exposure

[2] For α_1A280C only reaction with MTSES$^-$ had a functional effect, although MTSET$^+$ reacted. Thus, we measured the reaction rate with MTSES$^-$. We assume that the MTSET$^+$ reaction rate is ~10 times faster than that of MTSES$^-$ (29).

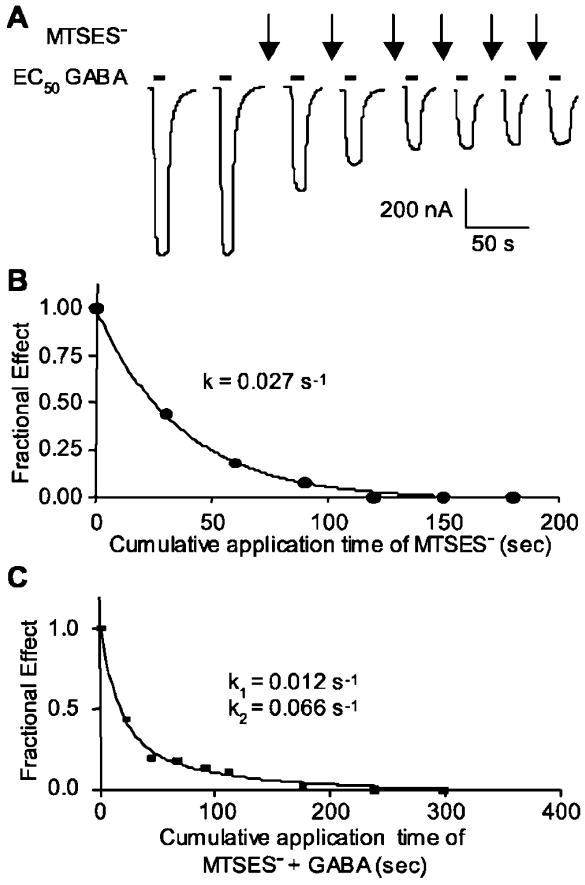

FIG. 7. **Measurement of MTSES$^-$ reaction rates with α_1A280C$\beta_1\gamma_2$ receptors.** *A*, EC$_{50}$ GABA test currents are shown. At each *downward arrow* 700 μM MTSES$^-$ was applied for 30 s. Each application of GABA or MTSES$^-$ was followed by a 3- to 5-min wash with CFFR buffer. *B*, normalized currents from the GABA-test pulses in *A* are plotted against cumulative exposure time to MTSES$^-$ and fitted with a single-exponential decay function. The pseudo-first order exponential decay constant, k, is given. *C*, measurement of the MTSES$^-$ reaction rate when applied in the presence of GABA to α_1A280C$\beta_1\gamma_2$ receptors. Normalized currents from the GABA-test pulses were fitted with a double-exponential decay function. This is the only mutant the required a double-exponential decay function to fit the data. The exponential decay constants, k_1 and k_2, are given. Average second order reaction rates are presented in Table II.

time *versus* percent change in current (Fig. 7) was best fit by a double-exponential equation (as judged by F-test, Prism). This gave two reaction rates (121 ± 38 and 695 ± 33 liters/mol-s, n = 3) with MTSES$^-$ in the presence of GABA. A possible explanation is that, in the presence of near-saturating GABA (5 times EC$_{50}$) there are two main populations of channels, *i.e.* desensitized and open. The two rate constants may reflect different MTSES$^-$ reaction rates with open and desensitized channels. Alternatively, there are two α subunits and thus two engineered Cys in each functional channel. If the accessibility of the two Cys was different, we might observe two reaction rates if reaction at each site contributed to the total effect.

DISCUSSION

We have shown that Cys substituted for all residues in the N-terminal portion of the M2–M3 loop between α_1Arg-273 and α_1Tyr-281, except α_1Pro-277, reacted with MTS reagents in the absence and in the presence of GABA. Based on the closed state MTSET$^+$ reaction rates these Cys mutants can be divided into two groups (Table II). The reaction rate of one group, which included α_1N274C, α_1S275C, α_1K278C, and α_1Y281C, was greater than 1000 liters/mol-s. The reaction rate of the other group, which included α_1R273C, α_1L276C, α_1V279C, and α_1A280C, was less than 300 liters/mol-s. On an α helical wheel plot the two groups of residues fall on opposite sides of the helix (Fig. 8*A*). The helical face containing the fast reacting residues is a direct continuation of the channel-lining face of the M2 segment (Fig. 8*B*) (13). The GABA$_A$ receptor M2 segment is largely α helical, based on SCAM experiments (13). Likewise, in ACh and 5-HT$_3$ receptors a variety of experiments imply that the M2 segment is largely α helical (6, 37–40). The M2 segment extracellular end is predicted, by amino acid sequence analysis, to lie near the 20′ position (α_1Asn-274), aligned with the extracellular ring of charge in the acetylcholine receptor (7, 8, 34, 41). Sequence analysis predicts that the residues beyond the 20′ position, in the M2–M3 loop, are in an extended structure (8). Our present experimental results suggest that the M2 segment α-helix extends beyond the predicted end of the M2 segment to include an additional two helical turns. The residues on the fast reacting face presumably line the wide, extracellular, channel vestibule. At present we do not know the position of these residues relative to the extracellular surface of the membrane.

We infer that MTS reagent access to the slow reacting side of the helix is restricted relative to the fast reacting side. The residues on the slow reacting face may interact with the lipid headgroup region of the bilayer or may interact with other parts of the protein. The identity of protein domains that might interact with the slow reacting face residues might include residues from other membrane-spanning segments or residues from the extracellular domain. Based on the high resolution crystal structure of the homologous acetylcholine binding protein, we can infer which extracellular domain residues may interact with the slow reacting face. In the crystal structure the pre-M1 region, the Cys loop, or the L1 loop are close to the membrane surface and, thus, may interact with the M2–M3 loop residues (12). The interaction with these other protein regions cannot be very tight. The MTS-reactive M2–M3 loop residues must, at least transiently, reach the water-accessible surface during the closed state to react with MTSET$^+$, because the MTS reagents react with ionized thiolate groups 10^9 times faster than with un-ionized thiols (42), and only water-accessible cysteines will ionize to any significant extent. Thus, MTS-reactive residues are, at least transiently, on the water-accessible protein surface. Several lines of evidence are consistent with the assumption that sulfhydryl reactivity is a measure of water-surface accessibility. In the aspartate chemotaxis receptor, a protein of known crystal structure, reactivity correlated with surface accessibility (43). More recently, the results of SCAM experiments on the dopamine D2 receptor correlated with surface accessibility of the aligned residues in the crystal structure of rhodopsin, a homologous G-protein-coupled receptor (44). Thus, even positions on the slow reacting helix face are, at least transiently, on the water-accessible protein surface to allow reaction with the MTS reagents. SCAM experiments in the homopentameric glycine receptor also reported that Cys substitution mutants in the N-terminal half of the M2–M3 loop were MTS-reactive (27). Similar differences in reaction rates, however, were not observed. In the case of the glycine receptor, each receptor has five engineered cysteines, one in each subunit, that may complicate the results because the conformation of each subunit may not be identical.

Alanine scanning mutagenesis of the N-terminal half of the M2–M3 loop showed effects on GABA EC$_{50}$ and efficacy only at α_1Arg-273 and α_1Leu-276, both on the slow reacting face (23). Another mutagenesis study showed that mutations of slow reacting face residues, α_1L276A, α_1P277A, and α_1Val279A, caused a right shift in the GABA EC$_{50}$ (24). Thus, it appears that mutation of slow reacting face residues has a greater effect

TABLE II
Average MTS reagent second-order reaction rate constants with the M2–M3 loop cysteine substitution mutants

Mutant	Reagent	Closed state[a]	n^b	+GABA[a]	n^b
R273C	$MTSET^+$	237 ± 13	3	371 ± 98[c]	3
N274C	$MTSET^+$	1878 ± 436	4	4961 ± 789[c]	3
S275C	$MTSET^+$	1160 ± 231	7	9743 ± 1281	5
L276C	$MTSET^+$			61 ± 7	4
K278C	$MTSET^+$	1163 ± 93	3		
V279C	$MTSET^+$	185 ± 62	4	1353 ± 91[c]	5
A280C	$MTSES^-$	28 ± 5	4	121 ± 38[c,d] 695 ± 33[c,d]	3
Y281C	$MTSET^+$	1067 ± 89	3	1023 ± 31	3
A284C	$MTSET^+$	39 ± 5	3	79 ± 7[c]	3

[a] Units are liters/mol-s, mean ± S.E.
[b] n = number of oocytes.
[c] Rate in the presence of GABA is significantly different from the rate in the absence of GABA.
[d] Unlike all other mutants, the data for this mutant in the presence of GABA were better fit by a double-exponential function.

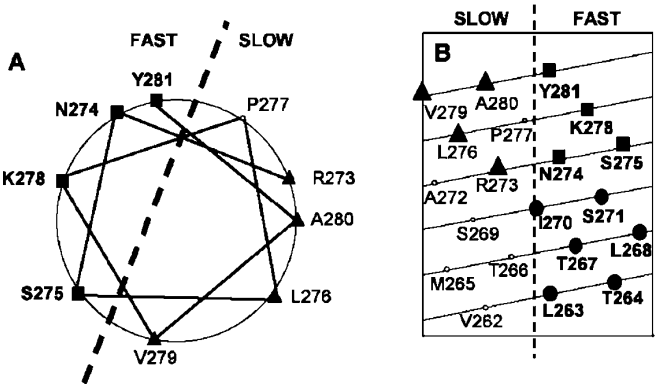

FIG. 8. **The residues at the extracellular end of the M2 segment and N-terminal portion of the M2–M3 loop are plotted on an α helical wheel (*A*) and an α helical net (*B*).** *A*, residues with $MTSET^+$ reaction rates > 1000 liters/mol-s are indicated by *black squares*. Residues with reaction rates < 300 liters/mol-s are indicated by *black triangles*. The *dashed line* separates the fast and slow reacting faces of the helix. Note that the fast reacting residues lie on one face of the helix. *B*, α helical net representation. The extracellular end is at the *top*. Residues that align vertically are on the same face of the helix. Channel-lining, sulfhydryl-reactive M2 segment residues for which reaction rates are not known are indicated by *black circles*. The channel-lining face residues are shown in *boldface type*. Note that the fast reacting residues lie on the same α helical face as the channel-lining residues. The *vertical dashed line* separates fast and slow reacting faces as in *panel A*.

on protein function than mutation of fast reacting face residues. An α helical secondary structure in this region of the M2–M3 loop, with one side facing the channel lumen and the other side interacting with protein or lipid, may help to explain the observation by Auerbach and colleagues (22). They found that hydrophobic mutations at adjacent positions in the ACh receptor α subunit M2–M3 loop had opposite effects on channel opening (22). Hydrophobic mutations at the position aligned with α_1Tyr-281, on the fast reacting face, increased the channel opening rate, whereas at the adjacent positions on the slow reacting face, aligned with $GABA_A$ α_1Val-279 and α_1Ala-280, hydrophobic mutations decreased the channel opening rate (22).

The highly conserved proline at the 23′ position lies on the slow reacting, non-channel-lining face of the helix. There was no evidence that the Cys substituted for it reacted with the MTS reagents (Figs. 4 and 5). We also tested for effects of other sulfhydryl reagents at this position, including *p*-chloromercuribenzenesulfonate ($pCMBS^-$) and MTS-tetramethylrhodamine, but neither had any effect (data not shown). Mutation of α_1Pro-277 to Cys caused a 14-fold increase in GABA EC_{50} and reduced the maximal currents. Mutation to alanine, however, was reported to decrease the GABA EC_{50} in one study using the α_2 subunit (23) and increase it in another that used the α_1 subunit (24). The mutated α_1P277C channels were still functional, suggesting that the proline is not essential for channel function. The marked effect of mutating the proline to Cys, and the lack of effect of application of the MTS reagents to this mutant, suggests that these reagents do not react with this engineered Cys, but we cannot rule out silent reaction. The proline may induce a bend in the helix in this region. The extent of a proline-induced bend is difficult to predict (45–48). This proline, or the structure of this region induced by the proline, may have a role in signal transduction from the extracellular ligand binding domain to the gate in the membrane-spanning domain. Perhaps α_1Pro-277 is in tight contact with another part of the protein, or the bend at this position may make the Cys inaccessible to the MTS reagents. We cannot distinguish these possibilities at present.

The $MTSET^+$ reaction rates could be measured both in the absence and presence of GABA at several of the Cys mutants. Reaction rates increased in the presence of GABA at positions on both sides of the helix. It should be remembered that in the presence of GABA the channel undergoes transitions between the open, desensitized, and closed states on a rapid time scale relative to our experiments. We do not know in which state(s) reaction is occurring in the presence of GABA. The GABA-induced rate increases indicate that this region undergoes a conformational change during gating. Increased reaction rates could result from changes in several factors, including: 1) the fractional time on the water-accessible surface could increase due to increased conformational mobility/flexibility, 2) local steric obstructions from neighboring residues or other parts of the protein could be reduced, and 3) changes in the local electrostatic potential could increase the ionization of the Cys or change the local concentration of $MTSET^+$. At present we cannot distinguish between these possibilities, although an electrostatic change affecting local MTS reagent concentration is the least likely, because $MTSES^-$ also reacted at these positions. At two positions, α_1R273C and α_1Y281C, GABA did not induce a significant increase in the $MTSET^+$ reaction rate.

Covalent modification of an engineered Cys can alter macroscopic GABA-induced currents by affecting the single channel conductance or channel gating kinetics. At most reactive positions modification by the positively and negatively charged reagents had similar functional effects, *i.e.* in most cases potentiation of subsequent submaximal GABA-evoked currents. Furthermore, MTS reagent modification of M2–M3 loop Cys mutants had little effect on currents evoked by saturating GABA concentrations.[3] Thus, we infer that the effects of modification on GABA-induced currents were not due to electro-

[3] A. K. Bera, M. Chatav, and M. H. Akabas, unpublished observations.

static interactions of the charge on the modified Cys with permeating ions. This implies that the potentiation due to covalent modification of the engineered Cys residues presumably results from a left shift in the GABA EC_{50} as we have observed previously in the M3 segment (33). In the absence of detailed single channel kinetic analysis of the effects of covalent modification at each position we do not know whether modification is affecting channel opening rates, closing rates, or desensitization rates. Furthermore, in the absence of a high resolution structure of the channel, it is not possible to provide a structural explanation for why covalent modification causes potentiation as opposed to inhibition. The problem is similar to the problem of interpreting the functional effects of mutagenesis experiments. Mutagenesis of some positions in this region alter GABA EC_{50} (23, 24, 49). One does not know whether these changes occur, because specific interactions between the mutated residue and other residues were altered or because the mutation caused a long range alteration in protein structure that altered function. Long range structural effects of mutagenesis have been reported. For example, in a crystallographic study of dihydrofolate reductase, a mutation 15 Å from the catalytic site caused less than a 1-Å deviation in the backbone structure resulting in a change in rotamer conformation of a residue in the catalytic site (50). There is no high resolution structural information on the extracellular end of the $GABA_A$ receptor channel. From the 9-Å resolution, cryo-electron microscopic images of the homologous ACh receptor the channel diameter in this region is about 20 Å (37). Charge change mutations in the ACh receptor at the M2 segment extracellular ring of charge, aligned with $GABA_A$ receptor α_1Asn-274, could not be explained by simple electrostatic effects on conductance (34, 51). In the *Drosophila* GABA receptor, the effects of mutations at the adjacent position, aligned with α_1Arg-273, were complicated suggesting that the effects arose from structural perturbations of the M2 segment (52). Thus, the conformation of this region may be sensitive to mutation. From disulfide cross-linking studies we inferred that there was considerable thermal motion in the extracellular ends of the M2 segments and this may extend into the M2–M3 loop residues (14). Covalent modification of residues in this region may alter the thermal motion and the conformational changes that this region undergoes during GABA-induced gating.

At two positions on the slow reacting face, α_1L276C and α_1A280C, both $MTSET^+$ and $MTSES^-$ reacted, but only one reagent caused a functional effect on subsequent GABA-induced currents, $MTSET^+$ at α_1L276C and $MTSES^-$ at α_1A280C (Figs. 4 and 5). Because these two MTS reagents are of comparable size and could fit in a right cylinder 10 Å long with a 6-Å diameter, it is likely that the functional effects of modification at these two positions are due to electrostatic interactions rather than steric effects. Although electrostatic forces seem to be important for the effects of modification at these two positions, they do not follow simple charge relationships and thus we do not believe that they result from interactions with permeating ions. If this region has an α helical secondary structure, the Cα carbons of these two residues would lie ~4.5 Å and ~10.5 Å above the Cα carbon of α_1Arg-273. Thus, the electrostatic interaction might be with this positively charged arginine or with another charged residue from elsewhere in the protein.

At two positions, α_1L276C and α_1K278C, $MTSET^+$ reacted in both the absence and presence of GABA but reaction only had a functional effect on the subsequent GABA-induced currents if it occurred in the presence of GABA at α_1L276C and in the absence of GABA at α_1K278C (Figs. 3 and 4). If $MTSET^+$ was applied sequentially in the absence and presence of GABA, then whichever condition $MTSET^+$ was applied first had the controlling effect on subsequent currents (Fig. 3). For example, if $MTSET^+$ was applied to α_1K278C in the presence of GABA, it had no functional effect. A subsequent application of $MTSET^+$ in the absence of GABA did not change the currents (Fig. 3*D*). However, if $MTSET^+$ were first applied in the presence of GABA, the subsequent currents were potentiated and a subsequent application of $MTSET^+$ in the absence of GABA had no effect on the potentiated currents. This implies that the engineered cysteines in both α subunits in each functional receptor complex were modified during the first application of $MTSET^+$, whether it was in the absence or in the presence of GABA. This prevented the subsequent application from having an effect. This implies that the conformations of the engineered Cys at positions 276 and 278 must be different in the closed and in the GABA-activated states. Once modified, the conformation is trapped, depending on whether the MTS reagent reacted in the absence or in the presence of GABA. The structural basis of this phenomenon is unclear, however, a similar effect was observed in the ACh receptor M2 segment at αS252C (38).

In the C-terminal half of the M2–M3 loop, from α_1Ala-282 to α_1Ile-289, there was only one MTS-reactive residue, α_1A284C. The reaction rate was less than 100 liters/mol-s (Table II). At the other positions there was no functional effect of MTS reagent application in either the absence or in the presence of GABA. We must interpret with caution results at positions where MTS reagent application had no effect, because there are two alternative explanations. One, the reagents did not react at a measurable rate either because the Cys is buried or local steric or electrostatic factors prevented access of the reagent and, two, the reagent did react but had no functional effect on GABA-induced currents (29). Our electrophysiological assay cannot distinguish between these possibilities. If these residues are buried they may be tightly interacting with other parts of the protein, such as the extracellular domain. Of note, the Cys mutants at positions α_1Asp-286 and α_1Phe-288 caused significant increases in GABA EC_{50} and reductions in the maximal GABA-induced currents compared with wild type (Table I). At α_1A282C only the maximal current was significantly affected by the mutation. As discussed above, in the absence of a high resolution structure it is difficult to discern the structural basis for these functional consequences of mutations.

In summary, our results suggest that the M2 segment α-helix extends two helical turns beyond the predicted end of the M2 segment. The channel-lining face of this region may help to line the wide extracellular channel vestibule. This region of the protein undergoes a conformational change during GABA-induced gating that increases the reactivity of Cys-substituted mutants. There were no functional consequences of MTS reagent application to Cys substituted for residues in the C-terminal end of the M2–M3 loop. This region may be tightly packed in the protein structure or covalent modification may be functionally silent. Further experiments will help to elucidate the role of this region in the transduction of GABA binding into opening of the transmembrane ion channel.

Acknowledgments—We thank Dr. Moez Bali, Dr. Jeff Horenstein, and Paul Riegelhaupt for helpful discussions and comments on this manuscript.

REFERENCES

1. Rabow, L. E., Russek, S. J., and Farb, D. H. (1995) *Synapse* **21,** 189–274
2. Ortells, M. O., and Lunt, G. G. (1995) *Trends Neurosci.* **18,** 121–127
3. Le Novere, N., and Changeux, J. P. (1999) *Nucleic Acids Res.* **27,** 340–342
4. Krasowski, M. D., and Harrison, N. L. (1999) *Cell Mol. Life Sci.* **55,** 1278–1303
5. Macdonald, R. L., and Olsen, R. W. (1994) *Annu. Rev. Neurosci.* **17,** 569–602
6. Karlin, A., and Akabas, M. H. (1995) *Neuron* **15,** 1231–1244
7. Schofield, P. R., Darlison, M. G., Fujita, N., Burt, D. R., Stephenson, F. A., Rodriguez, H., Rhee, L. M., Ramachandran, J., Reale, V., Glencorse, T. A.,

Seeburg, P. H., and Barnard, E. A. (1987) *Nature* **328,** 221–227
8. Le Novere, N., Corringer, P. J., and Changeux, J. P. (1999) *Biophys. J.* **76,** 2329–2345
9. Klausberger, T., Fuchs, K., Mayer, B., Ehya, N., and Sieghart, W. (2000) *J. Biol. Chem.* **275,** 8921–8928
10. Taylor, P. M., Connolly, C. N., Kittler, J. T., Gorrie, G. H., Hosie, A., Smart, T. G., and Moss, S. J. (2000) *J. Neurosci.* **20,** 1297–1306
11. Sieghart, W., Fuchs, K., Tretter, V., Ebert, V., Jechlinger, M., Hoger, H., and Adamiker, D. (1999) *Neurochem. Int.* **34,** 379–385
12. Brejc, K., van Dijk, W. J., Klaassen, R. V., Schuurmans, M., van Der Oost, J., Smit, A. B., and Sixma, T. K. (2001) *Nature* **411,** 269–276
13. Xu, M., and Akabas, M. H. (1996) *J. Gen. Physiol.* **107,** 195–205
14. Horenstein, J., Wagner, D. A., Czajkowski, C., and Akabas, M. H. (2001) *Nat. Neurosci.* **4,** 477–485
15. Eisele, J. L., Bertrand, S., Galzi, J. L., Devillers-Thiery, A., Changeux, J. P., and Bertrand, D. (1993) *Nature* **366,** 479–483
16. Mihic, S. J., Ye, Q., Wick, M. J., Koltchine, V. V., Krasowski, M. D., Finn, S. E., Mascia, M. P., Valenzuela, C. F., Hanson, K. K., Greenblatt, E. P., Harris, R. A., and Harrison, N. L. (1997) *Nature* **389,** 385–389
17. Vassilatis, D. K., Elliston, K. O., Paress, P. S., Hamelin, M., Arena, J. P., Schaeffer, J. M., Van der Ploeg, L. H., and Cully, D. F. (1997) *J. Mol. Evol.* **44,** 501–508
18. Ranganathan, R., Cannon, S. C., and Horvitz, H. R. (2000) *Nature* **408,** 470–475
19. Boileau, A. J., and Czajkowski, C. (1999) *J. Neurosci.* **19,** 10213–10220
20. Campos-Caro, A., Sala, S., Ballesta, J. J., Vicente-Agullo, F., Criado, M., and Sala, F. (1996) *Proc. Natl. Acad. Sci. U. S. A.* **93,** 6118–6123
21. Lynch, J. W., Rajendra, S., Pierce, K. D., Handford, C. A., Barry, P. H., and Schofield, P. R. (1997) *EMBO J.* **16,** 110–120
22. Grosman, C., Salamone, F. N., Sine, S. M., and Auerbach, A. (2000) *J. Gen. Physiol.* **116,** 327–340
23. O'Shea, S. M., and Harrison, N. L. (2000) *J. Biol. Chem.* **275,** 22764–22768
24. Davies, M., Newell, J. G., and Dunn, S. M. (2001) *J. Neurochem.* **79,** 55–62
25. Lewis, T. M., Sivilotti, L. G., Colquhoun, D., Gardiner, R. M., Schoepfer, R., and Rees, M. (1998) *J. Physiol.* (*Lond.*) **507,** 25–40
26. Rovira, J. C., Vicente-Agullo, F., Campos-Caro, A., Criado, M., Sala, F., Sala, S., and Ballesta, J. J. (1999) *Pflugers Arch.* **439,** 86–92
27. Lynch, J. W., Han, N. L., Haddrill, J., Pierce, K. D., and Schofield, P. R. (2001) *J. Neurosci.* **21,** 2589–2599
28. Akabas, M. H., Stauffer, D. A., Xu, M., and Karlin, A. (1992) *Science* **258,** 307–310
29. Karlin, A., and Akabas, M. H. (1998) *Methods Enzymol.* **293,** 123–145
30. Liman, E. R., Tytgat, J., and Hess, P. (1992) *Neuron* **9,** 861–871
31. Horenstein, J., and Akabas, M. H. (1998) *Mol. Pharmacol.* **53,** 870–877
32. Connolly, C. N., Krishek, B. J., McDonald, B. J., Smart, T. G., and Moss, S. J. (1996) *J. Biol. Chem.* **271,** 89–96
33. Williams, D. B., and Akabas, M. H. (1999) *Biophys. J.* **77,** 2563–2574
34. Imoto, K., Busch, C., Sakmann, B., Mishina, M., Konno, T., Nakai, J., Bujo, H., Mori, Y., Fukuda, K., and Numa, S. (1988) *Nature* **335,** 645–648
35. Miller, C. (1989) *Neuron* **2,** 1195–1205
36. Williams, D. B., and Akabas, M. H. (2000) *Mol. Pharmacol.* **58,** 1129–1136
37. Unwin, N. (1993) *J. Mol. Biol.* **229,** 1101–1124
38. Akabas, M. H., Kaufmann, C., Archdeacon, P., and Karlin, A. (1994) *Neuron* **13,** 919–927
39. Reeves, D. C., Goren, E. N., Akabas, M. H., and Lummis, S. C. (2001) *J. Biol. Chem.* **276,** 42035–42042
40. Changeux, J. P., and Edelstein, S. J. (1998) *Neuron* **21,** 959–980
41. Noda, M., Takahashi, H., Tanabe, T., Toyosato, M., Kikyotani, S., Furutani, Y., Hirose, T., Takashima, H., Inayama, S., Miyata, T., and Numa, S. (1983) *Nature* **302,** 528–532
42. Roberts, D. D., Lewis, S. D., Ballou, D. P., Olson, S. T., and Shafer, J. A. (1986) *Biochemistry* **25,** 5595–5601
43. Danielson, M. A., Bass, R. B., and Falke, J. J. (1997) *J. Biol. Chem.* **272,** 32878–32888
44. Ballesteros, J. A., Shi, L., and Javitch, J. A. (2001) *Mol. Pharmacol.* **60,** 1–19
45. Fu, D., Ballesteros, J. A., Weinstein, H., Chen, J., and Javitch, J. A. (1996) *Biochemistry* **35,** 11278–11285
46. Sansom, M. S., and Weinstein, H. (2000) *Trends Pharmacol. Sci.* **21,** 445–451
47. von Heijne, G. (1991) *J. Mol. Biol.* **218,** 499–503
48. Nilsson, I., and von Heijne, G. (1998) *J. Mol. Biol.* **284,** 1185–1189
49. Sigel, E., Buhr, A., and Baur, R. (1999) *J. Neurochem.* **73,** 1758–1764
50. Brown, K. A., Howell, E. E., and Kraut, J. (1993) *Proc. Natl. Acad. Sci. U. S. A.* **90,** 11753–11756
51. Kienker, P., Tomaselli, G., Jurman, M., and Yellen, G. (1994) *Biophys. J.* **66,** 325–334
52. Wang, C. T., Zhang, H. G., Rocheleau, T. A., French-Constant, R. H., and Jackson, M. B. (1999) *Biophys. J.* **77,** 691–700
53. Zhang, H., and Karlin, A. (1998) *Biochemistry* **37,** 7952–7964